Nutrition 38 (2017) 61–69

Contents lists available at ScienceDirect

Nutrition

journal homepage: www.nutritionjrnl.com

Basic nutritional investigation

Stereology shows that damaged liver recovers after protein refeeding

Silvio Pires Gomes Ph.D. [a], Andréa Almeida Pinto da Silva Ph.D. [a], Amanda Rabello Crisma Ph.D. [b], Primavera Borelli Ph.D. [b], Francisco Javier Hernandez-Blazquez Ph.D. [a], Mariana P. de Melo Ph.D. [c], Barbara Bacci Ph.D. [d], Andrzej Loesch Ph.D. [e], A. Augusto Coppi Ph.D. [d,*]

[a] Laboratory of Stochastic Stereology and Chemical Anatomy (LSSCA), Department of Surgery, College of Veterinary Medicine and Animal Science, University of São Paulo (USP), São Paulo, Brazil
[b] Laboratory of Haematology, Department of Clinical and Toxicologic Analyses, Faculty of Pharmaceutical Sciences, University of São Paulo (USP), São Paulo, Brazil
[c] Department of Basic and Environmental Sciences, Engineering School of Lorena, University of Sao Paulo (USP), Lorena, Brazil
[d] School of Veterinary Medicine, Faculty of Health and Medical Sciences, University of Surrey, Guildford, Surrey, United Kingdom
[e] Division of Medicine, University College London School of Life and Medical Sciences, Royal Free Campus, United Kingdom

ARTICLE INFO

Article history:
Received 3 August 2016
Accepted 18 February 2017

Keywords:
Liver
protein malnutrition
Mice
Stereology

ABSTRACT

Objective: The aim of the present study was to investigate the putative effects of a low-protein diet on the three-dimensional structure of hepatocytes and determine whether this scenario could be reversed by restoring the adequate levels of protein to the diet.
Methods: Using design-based stereology, the total number and volume of hepatocytes were estimated in the liver of mice in healthy and altered (by protein malnutrition) conditions and after protein renutrition.
Results: This study demonstrated a 65% decrease in the liver volume (3302 mm^3 for the control for undernourished versus 1141 mm^3 for the undernourished group) accompanied by a 46% reduction in the hepatocyte volume (8223 μm^3 for the control for undernourished versus 4475 μm^3 for the undernourished group) and a 90% increase in the total number of binucleate hepatocytes (1 549 393 for the control for undernourished versus 2 941 353 for the undernourished group). Reinstating a normoproteinic diet (12% casein) proved to be effective in restoring the size of hepatocytes, leading to an 85% increase in the total number of uninucleate hepatocytes (15 988 560 for the undernourished versus 29 600 520 for the renourished group), and partially reversed the liver atrophy.
Conclusions: Awareness of these data will add to a better morphologic understanding of malnutrition-induced hepatopathies and will help clinicians improve the diagnosis and treatment of this condition in humans and in veterinary practice.

Introduction

Protein–energy malnutrition (PEM) is a major form of malnutrition and is defined as an imbalance between food intake (protein and energy) and the amount that the body requires to ensure optimal growth and function [1,2]. PEM can cause delays in body maturation as well as affect neurologic and musculoskeletal system development [3].

To some extent, all tissues can be affected by a hypoproteinic state and the tissues most affected by protein deficiency are those that possess a high cellular turnover [4]. In the liver, protein malnutrition leads to altered liver biochemical characteristics and histology [5,6]. For instance, consumption of a protein-free diet (PFD) for 5 d changes the mouse liver proteome [7,8]. The mitochondrial DNA content of the liver is reduced in fetal and early postnatal malnourished rats even when proper nutrition was supplied after weaning [9].

This study was supported by São Paulo Research Foundation (FAPESP) and Conselho Nacional de Desenvolvimento Cientifico e Tecnologico (CNPq).
* Corresponding author. Tel./fax: +44 (0) 1483 68 44 55.
E-mail address: a.coppi@surrey.ac.uk (A. A. Coppi).

http://dx.doi.org/10.1016/j.nut.2017.02.010
0899-9007/

Despite the progress reported so far, knowledge of the mechanisms and pathogenesis of hepatocellular injuries of eating disorders is incomplete [5], and little is known as to the quantitative effects of a hypoproteinic diet on the three-dimensional (3-D) structure of hepatocytes and whether those effects can be reversed by renutrition with a normoproteinic diet.

Hence, in the present study we investigated the putative effects of a low-protein diet on the 3-D structure of hepatocytes in mice using design-based stereology and whether this scenario could be reversed by restoring the adequate levels of protein in the diet. Awareness of these data will add to a better morphologic understanding of malnutrition-induced hepatopathies and will help clinicians improve the diagnosis and treatment of this condition in humans and in veterinary practice.

Materials and methods

Animals

This study was approved by the Animal Care Committee of the School of Veterinary Medicine and Animal Science of the University of São Paulo. Livers were removed from 2-mo-old male Swiss mice (N = 20) obtained from the Department of Clinical and Toxicologic Analyses Animal Facility of the Faculty of Pharmaceutical Sciences of the University of São Paulo (USP) in Brazil. The animals were housed individually in metabolic cages under similar environmental conditions, with a 12-h light–dark cycle, temperature of 22 ± 2°C and relative humidity of 55 ± 10%. All animals fasted for 6 h and were supplied with water ad libitum. After acclimatization for 10 d to the diet (prepared in our laboratory, stored at −4°C until being administered and modified from the American Institute of Nutrition Recommendations for the Adult Rodent [AIN-93 M]) [10,11] the mice were systematically and randomly divided into two main diet groups: 10 mice receiving a normoproteinic diet (12% casein/energy) for 5 wk and 10 mice receiving a hypoproteinic diet (2% casein/energy) also for 5 wk. The full compositions of the diets used in this study are represented in Table 1.

When the experiment commenced, all 20 animals were 70 d old, and the mean (standard deviation [SD]) body weight was 41 g (1.9 g). After 5 wk, of the animals fed with a normoproteinic diet, five were sacrificed and used as a control for the undernourished group (CU) at the age of 105 d, whereas five were kept alive and received the same diet for an additional 5 wk as control for the renourished group (CR) at the age of 140 d. Similarly, of the mice fed with a hypoproteinic diet, five were sacrificed to represent the undernourished group (U), whereas the remaining five mice received a normoproteinic diet for an additional 5 wk; this was the renourished group (R). During the experiment, body weight and feed consumption were evaluated every 48 h. The denutrition protocol used here was similar to that previously published [11].

Biochemical tests

On day 105 for the U and CU groups, and on day 140 for the R and CR groups, animals were anesthetized with a combination of 120 mg/kg intramuscular ketamine chloride and 16 mg/kg intramuscular xylazine hydrochloride. Blood samples were obtained via brachial artery. Animals fasted for 6 h before blood collection.

Total protein, albumin, globulin, alanine aminotransferase (ALT), alkaline phosphatase (ALP), γ-glutamyl transpeptidase (GGT), aspartate aminotransferase (AST), and glucose plasma concentrations were measured with the Glucoquant assay (Roche Diagnostics GmbH, Mannheim, Germany) [12,13].

Sacrifice and histology

At specific group-related time points (day 105 or 140) animals were sacrificed with an intraperitoneal 100 mg/kg overdose of sodium pentobarbital (Bayer, Berlin). A bulbed cannula was inserted into the left ventricle of the heart of all mice; a cleansing solution of 0.1 M, pH 7.4 phosphate-buffered saline (PBS; Sigma, Berlin) containing 2% heparin (Roche) and 0.1% sodium nitrite (Sigma, Berlin) was injected via the ascending aorta; and a perfusion-fixation with 4% formaldehyde and 0.2% glutaraldehyde in PBS (0.1 M, pH 7.4) was conducted using a digital peristaltic perfusion pump with flux control of 6 mL/min. Subsequently, the abdominal cavity was incised by a midline incision (celiotomy) and the liver was identified, removed, weighed (wet weight), and immersed in the same fixative solution for 72 h at 4°C.

To produce vertical and uniform random (VUR) sections [14,15], livers were rotated along a vertical axis—normal to the organ—and embedded in a 10% agar solution, and exhaustively sectioned with a nominal thickness of 40 μm using a VT1000 S vibratome (Lieca Biosystems, Wetzlar, Germany). Sections were collected onto glass slides, stained with Mayer's hematoxylin (Merck, Berlin) and mounted under a coverslip with a drop of DPX (Fluka, Hanover). Section images were acquired using a DMR Leica microscope equipped with a High-End DP 72 Olympus digital camera (using either ×40 or ×63 oil lenses) and projected onto a computer monitor. Stereological analyses were performed using the newCAST Visiopharm stereology system version 4.4.4.0 (Visiopharm, Copenhagen, Denmark).

Table 1
Full composition of the normoproteinic and hypoproteinic diets administered to the mice used in this study

Ingredients	Normoproteinic diet (g/kg diet)*	Hypoproteinic diet (g/kg diet)*
Casein (>85%)†	120	20
Sucrose	100	100
Fiber	50	50
Soybean oil	40	40
Mineral mix‡	35	35
Vitamin mix§	10	10
L-cystin	1.8	0.3
Choline bitartrate	2.5	2.5
Cornstarch	640.7	742.2
Tert-butylhydroquinone	0.008	0.008

* Both diets were prepared in our laboratory, and their composition was according to AIN-93 M rodent diet.
† Casein supplied by Labsynth (Brazil).
‡ Mineral mix supplied by Rhoster Indústria e Comércio LTDA (Brazil) (mineral mix for AIN-93 M rodent diet).
§ Vitamin mix supplied by Rhoster Indústria e Comércio LTDA (Brazil) (vitamin mix for AIN-93 M rodent diet).

Liver volume, V_{LIV}

The total volume of the liver was estimated by means of the Cavalieri principle [16] in the same reference sections used for disectors. Briefly, liver agar-embedded blocks were exhaustively serially sectioned and every 12th section was sampled and measured for cross-sectional area. Then,

$V_{LIV} := T \times \sum A_{LIV}$,

Where T is the between-section distance (480 μm) and $\sum A_{LIV}$ is the sum of the delineated profile areas of the chosen set of liver sections. Profile areas were estimated from the numbers of randomly positioned test points (~300 per liver) hitting the whole reference space and the areal equivalent of a test point.

Shrinkage estimation

Liver fragments were then dissected out, weighed, and their wet weights were converted into volumes using a tissue density of 1.06 g/cm^3 for estimating tissue distortion (shrinkage). Tissue density had been previously estimated in a pilot study, with mice treated with similar conditions, by simply weighing livers and dividing their wet weights (g) (after perfusion-fixation) by their volumes (cm^3) estimated by liquid displacement [17]. Mean tissue densities and their coefficients of variation (CVs) in the groups were 1.059 g/cm^3 (0.10; CU group), 1.061 g/cm^3 (0.09; U group), 1.060 g/cm^3 (0.10; R group), and 1.059 g/cm^3 (0.10; CR group). Because intergroup differences did not attain significance ($P = 0.44$), the same tissue density (i.e., 1.06 g/cm^3) was used for all study groups to estimate tissue shrinkage.

The mean volume shrinkage (CV expressed as a decimal fraction of the mean) was estimated to be 3.8% (0.20) in the U group, 3.4% (0.22) in the CU group, 3.1% (0.21) in the R group, and 3.9% (0.18) in the CR group. No correction for global shrinkage was performed as between-group differences were not significant ($P = 0.231$).

Total number of hepatocytes: N_{HEP}

The optical fractionator was used for estimating the total number of uninucleate and binucleate hepatocytes (N_{HEP}) [16,18]. Each liver agar-embedded block was exhaustively serially sectioned into 40-μm-thick sections and a mean sampling fraction (ssf)—1/28 for CU; 1/36 for U; 1/47 for R, and 1/33 for CR groups—of these sections was selected. Before starting the counting procedure, a z-axis distribution was performed to:

1. Determine the hepatocyte distribution throughout section thickness;
2. Determine the Mayer's hematoxylin-hepatocyte staining penetration throughout section thickness; and
3. Establish the disector height, which was 19 μm for CU and U, and 15 μm for R and CR groups.

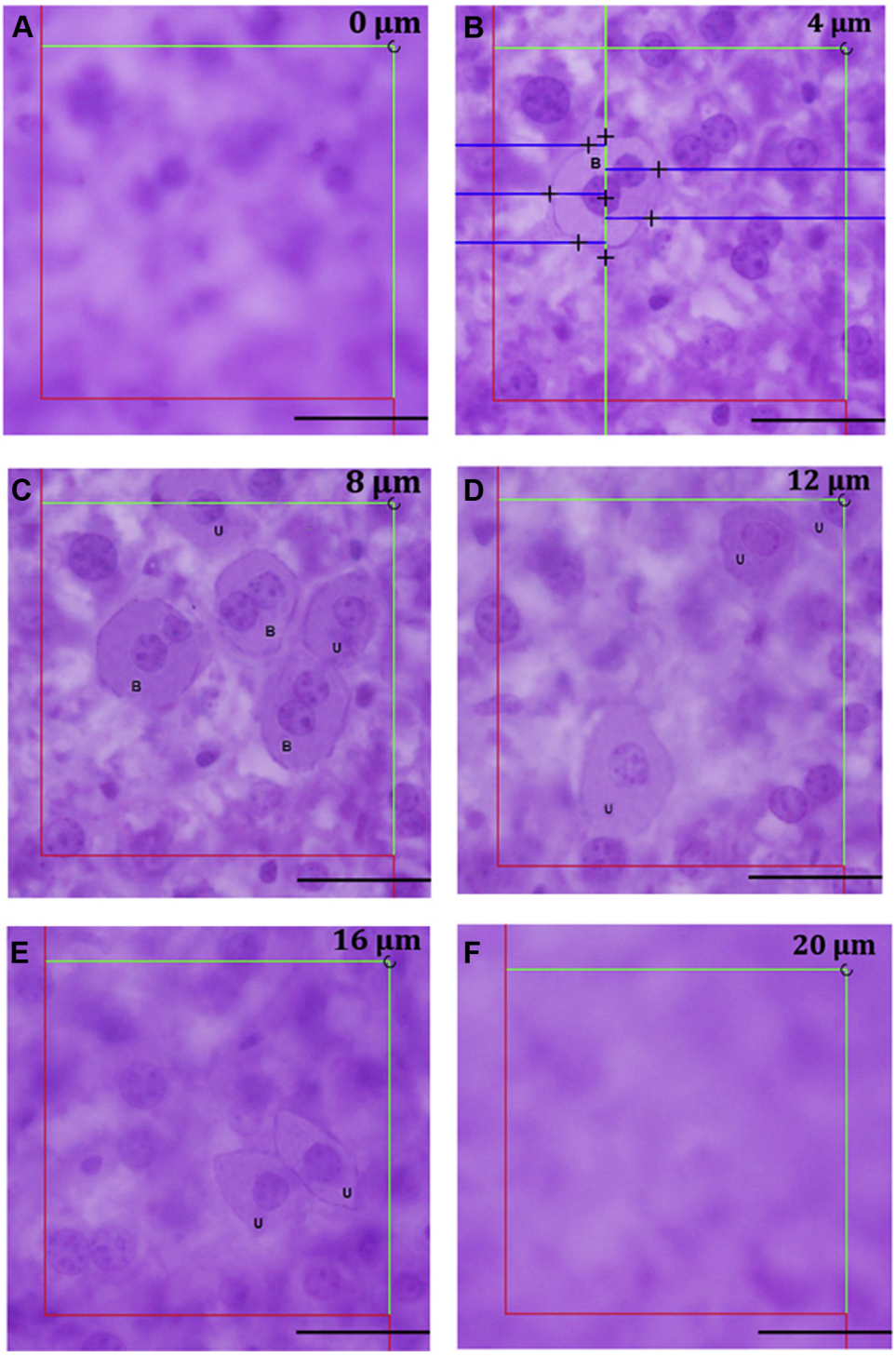

Fig. 1. Images of successive focal planes throughout a Mayer's hematoxylin-stained optical section of a mice liver from the renourished group illustrating the application of the optical disector. The distance between each focal plane is 4 µm. On plane A (uppermost surface of the section), a field of view, selected using an unbiased counting frame, is followed along the whole section thickness (planes B, C, D, E, and F), and hepatocytes are sampled and counted as they come into focus on each focal plane. For instance, on plane C (8 µm apart from plane (A) two uni- (U) and three binucleate (B) hepatocytes are sampled. The uninucleate hepatocyte in the upper left corner of the unbiased counting frame is not sampled as its cell membrane touches the exclusion line. The lowermost focal plane (F; bottom surface of the section) is 20 µm apart from plane A, and no particles are sampled on it. Scale bars: 30 µm.

Section thickness was measured in every field of view using the central point of the unbiased counting frame.

To avoid putative bias in the differentiation between uninucleate and binucleate hepatocytes attributed to a nonuniform penetration of Mayer's hematoxylin staining, it was always checked in every field of view that Mayer's hematoxylin staining penetration would be ≥30 µm from the uppermost section plane. Therefore, we worked with upper and lower guard zones of 5 and 16 to 20 µm, respectively.

The mean height sampling fraction (hsf) was 1/2 and the entirely hepatocyte was defined as the counting unit, regardless of its nuclei number (Fig. 1).

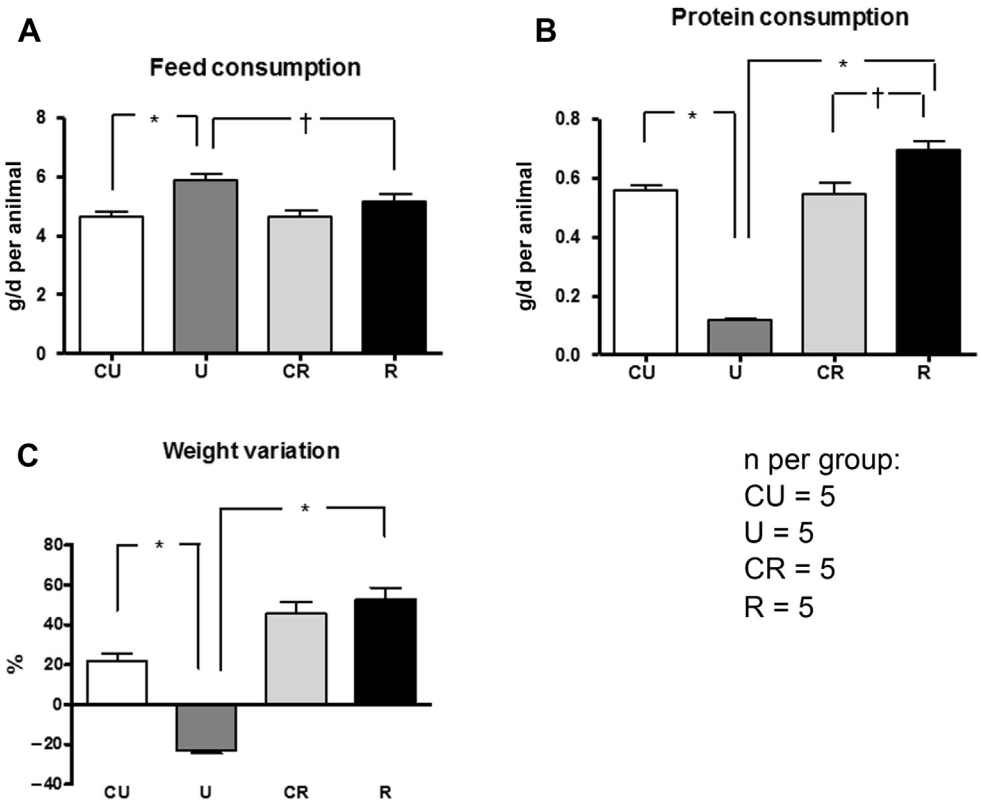

Fig. 2. Mean diet consumption (g/d for each animal) (A), mean protein consumption (g/d for each animal) (B), and animal body weight range (%) in the experimental groups (C). The number of animals studied in the control for the undernourished (CU), undernourished (U), renourished (R), and control for the renourished (CR) groups is represented by N. $^{*}P \leq 0.005$. $^{\dagger}P \leq 0.05$.

A mean area sampling fraction (asf) of 1/504 of the chosen liver sections was sampled using two-dimensional unbiased counting frames [19] with a frame area equivalent to 5.074 μm^2. In the control for the undernourished group, 86 disectors were applied to count 420 hepatocytes ($\sum Q^-$). In the undernourished group an average of 97 disectors were used to count 432 hepatocytes. In the renourished group, 94 disectors were applied to count 625 hepatocytes. Finally, in the control for the renourished group, 96 disectors were applied to count 596 hepatocytes.

The total number of hepatocytes was then estimated by multiplying the counted number of particles ($\sum Q^-$)—sampled using disectors—by the reciprocal of the above-stated sampling fractions:

$$N_{HEP} = ssf^{-1} \times hsf^{-1} \times asf^{-1} \times \Sigma Q^-$$

Hepatocyte volume: $\bar{v}_{N_{HEP}}$

The mean volume of hepatocytes was estimated by the planar rotator method [20], which is a local and direct estimator of particle volume and uses the disector as a sampling probe. In the present study, the planar rotator was computer assisted using the six half-line rotator probe available in the newCAST Visiopharm stereology system (version 4.4.4.0.) and in the same reference sections used for total number estimation (Fig. 1).

Statistical analyses

The precision of a stereologic estimate was expressed as a coefficient of error (CE) calculated as described elsewhere [21]. In the Results section, the whole data were expressed as group mean (observed CV [CV_{obs}]) where CV_{obs} represents SD/mean. Group differences were assessed by either one-way analysis of variance (ANOVA) or Mood's Median Test using Minitab version 17. When using one-way ANOVA and in the event of significant between-group differences ($P < 0.05$), we applied Tukey's test for multiple comparisons.

Results

Clinical examination

General symptoms of malnutrition were present in the undernourished mice (e.g., skin folds, mucosa opacity, and body weight loss). Additionally, edema and fluid accumulation were seen in serous cavities.

Food, protein consumption, and body weight

Although the U group had a higher diet consumption compared to the CU group, this increase did not lead to a rise in protein consumption; in fact the consumption of this nutrient was lower in the U group (Fig. 2). In the R group, the consumption of diet and protein resumed to normal values and was higher than in the CR group. In relative terms, the consumption of protein per unit of body weight (g/g of body weight) was 0.012 (0.10) in the CU group, 0.003 (0.15) in the U group, 0.012 (0.19) in the R group, and 0.014 (0.13) in the CR group. With the exception of mice from the U group ($P = 0.01$) mice from the other three groups (CU, R, and CR) had the same consumption of protein per unit of body weight (g/g of body weight).

At the end of the experiment, the body weight of the animals of the U group was reduced by 23% compared with their initial body weight. Conversely, the body weight of animals of the CU group increased by 20%. Finally, mice from the R group presented an increase of about 70% compared with their body at the beginning of the nutritional rehabilitation, whereas mice from the CR group presented an increase of about 40% in relation to their initial body weight. Body weight variation for CU, U, and CR groups was calculated considering mice body weight at the beginning of the denutrition protocol. Body weight variation for the R group, however, was calculated considering mice body weight at the beginning of the nutritional recovery protocol (i.e., the body weight animals presented after 5 wk consuming a hypoproteinic diet; Fig. 2).

Table 2
Biochemical parameters in mice from control for the undernourished (CU), undernourished (U), renourished (R), and control for the renourished (CR) groups

Biochemical parameters	Groups				*P*
	CU	U	R	CR	
Total protein, g/dL	5.4^{A} (0.05)	5.18^{B} (0.11)	5.96^{A} (0.07)	5.92^{A} (0.03)	0.03*
Albumin, g/dL	2.18^{A} (0.04)	1.75^{B} (0.06)	2.12^{A} (0.05)	2.2^{A} (0.02)	0.02*
Globulin, g/dL	2.4^{A} (0.07)	2.1^{A} (0.20)	2.2^{A} (0.09)	2.23^{A} (0.07)	0.60
Alanine aminotransferase, U/L	44.3^{A} (0.30)	9.0^{A} (0.30)	13.33^{A} (0.25)	41^{A} (0.32)	0.074
Alkaline phosphatase, U/L	106^{A} (0.11)	414^{B} (0.38)	147.7^{A} (0.17)	$159.3^{A,B}$ (0.04)	0.021*
γ-glutamyl transpeptidase, U/L	0.33^{A} (0.17)	1.33^{A} (0.11)	0.22^{A} (0.12)	0.22^{A} (0.12)	0.227
Aspartate aminotransferase, U/L	105.3^{A} (0.38)	135^{A} (0.37)	100^{A} (0.21)	126.3^{A} (0.16)	0.591
Glucose, mg/dL	178^{A} (0.19)	76.7^{B} (0.20)	117^{A} (0.29)	156^{A} (0.07)	0.02*

Values are group means (coefficients of variation). Means that do not share the same superscript letter (A or B) are significantly different
* Indicates significance.

Biochemical tests

Total protein, albumin, globulin, ALT, ALP, GGT, AST, and glucose plasma concentrations are summarized in Table 2. There were significant changes in the glucose, alkaline phosphatase, albumin, and total protein levels.

Liver volume: V_{LIV}

The stereologic data were collated in form of a table (Table 3). The volume of the liver amounted to 3302 mm^3 (0.05) in the CU group, 1141 mm^3 (0.06) in the U group, 2870 mm^3 (0.06) in the R group, and 3925 mm^3 (0.05) in the CR group. Apparent intergroup differences were significant ($P = 0.0001$; i.e., each group presented noticeable differences from the others; Fig. 3, Table 3). The precision of liver volume estimation—expressed as CE (V_{LIV})—was 0.015 in the CU group, 0.017 in the U group, 0.012 in the R group, and 0.0102 in the CR group.

Additionally, liver weights were 3.5 g (0.06) in the CU group, 1.21 g (0.05) in the U group, 3.04 g (0.06) in the R group, and 4.16 g (0.05) in the CR group. Apparent intergroup differences were significant ($P = 0.001$). In relative terms, the liver weight per unit of body weight (g/g of body weight) was 0.040 (0.12) in the CU group, 0.041 (0.15) in the U group, 0.047 (0.12) in the R group, and 0.045 (0.13) in the CR group. In mice from all four groups, liver weights represented the same proportion per unit of body weight ($P = 0.338$).

Total number of hepatocytes: N_{HEPuni} and N_{HEPbi}

The total number of uninucleate hepatocytes was 11 874 280 (0.07) for the CU group, 15 988 560 (0.08) for the U group, 29 600 520 (0.13) for the R group, and 19 995 200 (0.20) for the CR group. The R group data were different from the other three groups ($P = 0.015$; Table 3). The precision of number of uninucleate hepatocytes estimation—expressed as CE (N_{HEPuni})—was 0.02 for the CU group, 0.03 for the U group, 0.03 for the R group, and 0.04 for the CR group.

The total number of binucleate hepatocytes was 1 549 393 (0.14) for the CU group, 2 941 353 (0.21) for the U group, 3 070 816 (0.20) for the R group, and 1 536 403 (0.23) for the CR group. Data from the U and R groups were different from those of CU and CR groups ($P = 0.005$; Table 3). The precision of number of binucleate hepatocytes estimation—expressed as CE (N_{HEPbi}) was 0.03 for the CU group, 0.05 for the U group, 0.03 for the R group, and 0.02 for the CR group.

Hepatocyte volume: $\overline{v}_{N_{HEP}}$

The mean volume of hepatocytes was 8223 μm^3 (0.07) for the CU group, 4475 μm^3 (0.05) for the U group, 8011 μm^3 (0.02) for the R group, and 10 003 μm^3 (0.05) for the CR group. The mean hepatocyte volume provided here is an average between uninucleate and binucleate hepatocytes' volumes. Data from the U group or from the CR group were different from the other groups ($P = 0.001$; Table 3, Fig. 4).

Discussion

Biochemical markers of liver function

In the undernourished group, the hypoproteinic diet led to an important reduction in albumin (20%)—the concentration of albumin is an excellent gauge of liver protein synthesis [22,23] and marker of nutritional status [24,25].

Another important finding was the 291% increase in the ALP concentration in the undernourished group. ALP is an enzyme that transports metabolites across cell membranes and is present on the surface of bile duct epithelia. Cholestasis and the accumulation of bile salts enhance the synthesis and release of ALP from the cell surface. ALP levels usually rise late in bile duct obstruction and drop slowly after resolution [22,26]. We hypothesize that protein malnutrition (2% casein) may have damaged the structure of intrahepatic biliary ductal system augmenting the concentration of ALP, which was reversed when a normoproteinic diet (12% casein) was reinstated to the animals.

Table 3
Stereological parameters in mice from control for the undernourished (CU), undernourished (U), renourished (R), and control for the renourished (CR) groups

Stereological parameters	Groups				*P*
	CU	U	R	CR	
Liver volume, mm^3	3302^{A} (0.05)	1141^{B} (0.06)	2870^{C} (0.06)	3925^{D} (0.05)	0.0001
Total number of uninucleate hepatocytes	$11\ 874\ 280^{A}$ (0.07)	$15\ 988\ 560^{A}$ (0.08)	$29\ 600\ 520^{B}$ (0.13)	$19\ 995\ 200^{A}$ (0.20)	0.015
Total number of binucleate hepatocytes	$1\ 549\ 393^{A}$ (0.14)	$2\ 941\ 353^{B}$ (0.21)	$3\ 070\ 816^{B}$ (0.20)	$1\ 536\ 403^{A}$ (0.23)	0.005
Hepatocyte volume, μm^3	8223^{A} (0.07)	4475^{B} (0.05)	8011^{A} (0.02)	$10\ 003^{C}$ (0.05)	0.001

Values are group means (coefficients of variation). Means that do not share the same superscript letter (A, B, C, or D) are significantly different

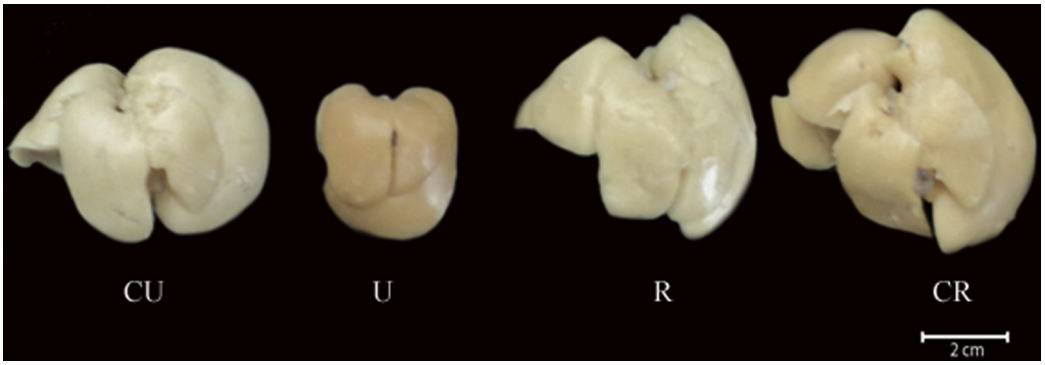

Fig. 3. Macroscopic images of the mice liver from the control for the undernourished (CU), undernourished (U), renourished (R), and control for the renourished (CR) groups depicting startling differences in their sizes (i.e., protein-deficient diet led to a serious liver atrophy: 65% reduction in liver volume of undernourished animals, which was not reversed with protein refeeding). Scale bar: 2 cm.

Because the minimum daily amounts of all nutrients (but protein) were ingested by the animals in the malnourished group, we concluded that the changes observed in the present experimental model were mainly the result of the reduction in protein and energy intake compared with the control group.

Liver stereology

In this study, design-based stereology was used to monitor the effects of a hypoproteinic diet on the structure of mice liver and to determine whether those effects could be reversed by refeeding the animals with a normoproteinic diet.

The most startling finding of the present study was just how damaging protein malnutrition is: There was a 65% decrease in the liver volume accompanied by a 46% reduction in the hepatocyte volume and a 90% increase in the total number of binucleate hepatocytes. The hypoproteinic diet (2% casein) in the present study led to severe organ and cell atrophy (i.e., both liver and hepatocytes were reduced to about half their initial size).

Before we started this experiment, we had hypothesized that protein refeeding would reverse the deleterious effects on the structure of the liver; this proved to be partially correct. The normoproteinic diet (12% casein) was effective in restoring the volume of hepatocytes but failed, nonetheless, to completely reverse the liver atrophy characterized by the reduction of the liver volume. (For more details, see the section on liver and hepatocyte volume.) The active participation of the connective tissue in liver diseases, such as cirrhosis, is well established [27], and although we have not measured this structural component of the liver, it is possible that a reduction in liver connective tissue could be one of a plethora of other factors contributing to

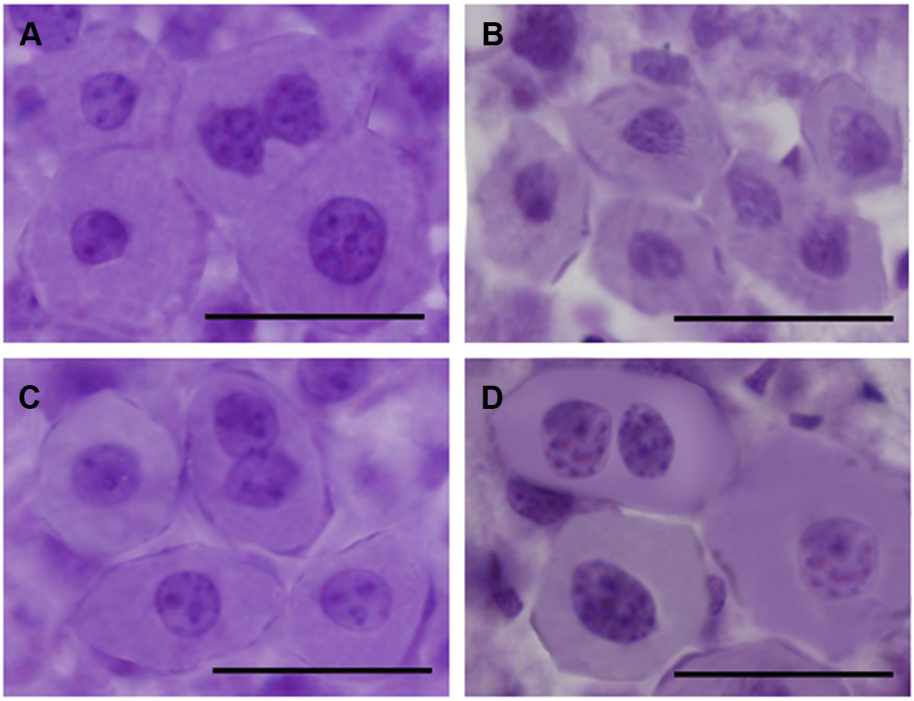

Fig. 4. Light-microscopic images of Mayer's Hematoxylin-stained optical sections of a mice liver from the control for the undernourished (A), undernourished (B), renourished (C), and control for the renourished (D) groups depicting details of the liver microstructure. Protein-deficient diet led to serious hepatocyte atrophy, 46% reduction in the cell volume (B), which was reversed with protein refeeding (R). Scale bars: 30 μm.

the organ atrophy observed in the present study. Other factors potentially involved in liver atrophy are discussed later.

Total number of hepatocytes

Methodological considerations

In the present study, the entire hepatocyte was defined as the counting unit, regardless of its nuclei number. When perusing the relevant literature, we noticed that authors have mainly used four different stereologic approaches to count hepatocytes. The approaches are as follow:

1. Using the nuclei as the counting unit and therefore estimating the total number of hepatocyte nuclei and yet not providing the total number of hepatocytes [28].
2. Using the nuclei as the counting unit, estimating the numerical density of uni- and binucleate hepatocytes and then multiplying these data (numerical density of hepatocyte nuclei) by the liver volume [29]. (We argue that this approach would suggest that the authors assumed that the number of hepatocyte nuclei equals the total number of hepatocytes themselves and, if so, we do not agree with this approach.)
3. Using the nuclei as the counting unit and discriminating between uni- and binucleate hepatocytes in 5-μm-thick physical sections, taking into account a correction based on the mean nucleus height of hepatocytes, which again assumes that the distribution of hepatocytes' nuclei heights is the same in the whole liver [30].
4. Using the aid of immunohistochemistry techniques, that is, using polyclonal antibodies against carcinoembryonic antigen (CEA) and, because biliary canaliculi are then marked, the authors advocate that an "unequivocal" counting of uninucleate and binucleate hepatocytes was achieved [31].

Although we welcome the association between immunohistochemistry and stereology, CEA is not a specific labelling for hepatocytes and yet it is directed against biliary canaliculi as previously mentioned [31] and primarily useful for the study of hepatoblastomas [32]. Therefore, we postulate that an unequivocal identification of uni- and binucleate hepatocytes would not have been accomplished solely based on the use of CEA.

Therefore, we can identify advantages and disadvantages in every technique, including ours, and we always aim at producing an accurate and precise estimation of parameters with a lower and acceptable coefficient of error, which we think was attained in the present study. Additionally, we think the association of perfusion-fixation achieved by using a digital peristaltic perfusion pump with flux control of 6 mL/min with the generation of VUR sections (the former was important in leading toward an workable tissue fixation, whereas the latter was important to elicit a more uniform penetration of Mayer's hematoxylin-hepatocyte staining) was important. Indeed, as with Mayer's hematoxylin [33], hepatocyte staining was highly appropriate for the identification of hepatocytes as it allowed for a clearly distinguishable cell membrane against the background of the histologic section.

Ultimately, the use of immunohistochemistry was not necessary to render a reliable identification and counting of uninucleate and binucleate hepatocytes, which was always pursued by the same experienced person.

Our estimates for the total number of uninucleate hepatocytes in the mice liver are 99% lower than that reported for the rat liver in a study that employed the optical disector [31] and in another study that elicited data by means of the physical dissector [34]. The mice used in the present study weighed 85% less than the rats investigated in Marcos et al.'s study [31], which demonstrated a positive correlation between animal body weight and the number of binucleate hepatocytes. Using the optical dissector, the total number of hepatocyte nuclei was estimated in bulb-c mice to be 5.3×10^8 [28]. Unfortunately, the aforementioned authors [28] did not report on the total number of hepatocytes, which would have allowed for a direct comparison with our data in the same species (i.e., mice).

In the present study, there was a 90% increase in the total number of binucleate hepatocytes and protein malnutrition exerted no effects on the total number of uninucleate hepatocytes. Conversely, protein refeeding indeed led to an 85% increase in the total number of uninucleate hepatocytes. The proportion of binucleate to uninucleate hepatocytes was 13% in the control for the undernourished group; increased to 18% in the undernourished group, explained by the 90% increase in the number of binucleate hepatocytes; subsequently reduced to 10.4% in the renourished group, explained by the 85% increase in the number of uninucleate hepatocytes; and finally reached 7.7% in the control for the renourished group. Similarly, very recently, it has been demonstrated that the administration of a proteinic parenteral solution of hepatotrophic factors in partially hepatectomized rats led to a 44.9% rise in the hepatocyte proliferation rate increasing the liver regenerative capacity [35].

Although we have not used cell proliferation markers such as Ki-67, we have robust 3-D design-based stereology conducted estimations sufficient enough to believe that the 90% increase in the total number of binucleate hepatocytes in the undernourished group (U) do represent hepatocellular proliferation and the latter could be explained by the fact that those cells play an important role in hyperplastic liver reaction (liver plasticity), acting as a cell reservoir for rapid liver regeneration [36,37] and producing uninucleate hepatocytes through an amitotic cytokinesis [38].

An increase in the proportion of uninucleate hepatocytes generally follows a decrease in the percentage of binucleate hepatocytes. This has been constantly reported in response to dimethylaminobenzene- [37] and iethylnitrosamine/phenobarbitone-induced [39] hepatocarcinogenesis. By contrast, in the undernourished group, the total number of binucleate hepatocytes in fact rose by 90% due to protein malnutrition and yet this was not accompanied by an increase in the total number of uninucleate hepatocytes as seen previously [38]. Despite all hypotheses published in the literature, the functional role of binucleation in hepatocytes, which starts before 3 wk of postnatal life (day 14), is still unclear, complex, and has a multifactorial onset. Just in 2016, microRNAs (miR-122) have been involved in triggering hepatocyte binucleation in mice [40].

Liver and hepatocyte volume

Liver and hepatocyte volumes were estimated in bulb-c mice [28]. Bulb-c mice hepatocytes are 55% smaller than those of the Swiss mice we used, and their livers are twofold smaller. Regarding the hypoproteinic diet used in the present study, this led to a 65% decrease in the liver volume accompanied by a 46% reduction in the hepatocyte volume (i.e., organ and cell atrophy, respectively).

We hypothesize that the 65% reduction in the liver volume of undernourished mice could be caused by the 46% reduction in hepatocyte volume that was triggered by lower protein

availability in the diet and its induced damage to the hepatocyte structure. Other liver structural units such as the biliferous and vascular system also could be reduced and play an additional role in liver atrophy, although we have not measured them. Along similar lines, Parra et al. [41] have shown a 27.4% reduction in liver mass in rats subject to PEM that was attributed to two factors: a decrease in hepatocyte number (hypoplasia), which has not been confirmed by our data, and reduction in the size of hepatocytes (atrophy), which has been shown in our study. According to two studies [41,42], liver and hepatocyte atrophy was caused by reduction in the flow of hepatotrophic factors (such as insulin) to the liver after prolonged lack of food ingestion.

It also is interesting to observe the dynamic relationships between the liver and its compartment units. For instance, if the liver size is reduced by 65% in undernourished mice, how could the organ accommodate simultaneously a 90% increase in the total number of binucleate hepatocytes? The answer may rest on the fact that there was a 46% reduction of cell size (hepatocyte volume), that is, we could be observing a compensatory regenerative mechanism related to liver plasticity characterized by a high proliferation rate of smaller binucleate hepatocytes that are now allocated in a smaller (atrophied) organ. Similarly, when one compares the control group for renourished mice with the control group for the undernourished animals, the liver volume of the former is 19% bigger than the latter. This change occurred in conjunction with a 22% increase in the hepatocyte volume (cell hypertrophy) in the control for the renourished group. Therefore, we suggest that hepatocyte hypertrophy could be one of the main causes of liver hypertrophy seen in this group and yet we cannot rule out that other structural components of the liver such as vascular and biliferous systems as well as the connective tissue also could be implicated in this structural change.

Additionally, the liver volume of the renourished group is only 13% less than the liver of the control for the undernourished group. Because our renutrition protocol with a normoproteinic diet lasted for 5 wk, we strongly believe that liver volume would have been restored to normal values had the renutrition protocol been expanded for at least an additional week, as was the case for hepatocyte volume, which was restored to normal values after refeeding subjects with a normoproteinic diet after 5 wk.

Conclusions

The present study adds to the understanding of protein malnutrition-induced damage to the liver structure. Subsequent lines of research inquiry would be the investigation into the molecular mechanisms governing hepatocyte size recovery and the possible role played by binuclate hepatocytes during protein refeeding-induced liver regeneration. We hope that the results elicited by the present study can be translated into improving the dietary conditions for populations worldwide, especially for those individuals living in poor and developing countries.

References

[1] Fock RA, Rogero MM, Vinolo MA, Curi R, Borges MC, Borelli P. Effects of protein–energy malnutrition on NF-kappaB signalling in murine peritoneal macrophages. Inflammation 2010;33:101–9.

[2] Bossola M. Nutritional interventions in head and neck cancer patients undergoing chemoradiotherapy: a narrative review. Nutrients 2015;7:265–76.

[3] Mayneris-Perxachs J, Bolick DT, Leng J, Medlock GL, Kolling GL, Papin JA, et al. Protein- and zinc-deficient diets modulate the murine microbiome and metabolic phenotype. Am J Clin Nutr 2016;104:1253–62.

[4] Deo MG. Biology of protein-calorie malnutrition. World Rev Nutr Diet 1978;32:49–95.

[5] Caballero VJ, Mendieta JR, Lombardo D, Saceda M, Ferragut JA, Conde RD, et al. Liver damage and caspase-dependent apoptosis is related to protein malnutrition in mice: effect of methionine. Acta Histochem 2015;117:126–35.

[6] Feres NH, Reis SR, Veloso RV, Arantes VC, Souza LM, Carneiro EM, et al. Soybean diet alters the insulin-signaling pathway in the liver of rats recovering from early-life malnutrition. Nutrition 2010;26:441–8.

[7] Sanllorenti PM, Rosenfeld J, Ronchi VP, Ferrara P, Conde RD. Two dimensional non equilibrium pH gel electrophoresis mapping of cytosolic protein changes caused by dietary protein depletion in mouse liver. Mol Cell Biochem 2001;220:49–56.

[8] Ronchi VP, Giudici AM, Mendieta JR, Caballero VJ, Chisari AN, Sanllorenti PM, et al. Oxidative stress in mouse liver caused by dietary amino acid deprivation: Protective effect of methionine. J Physiol Biochem 2010;66:93–103.

[9] Park KS, Kim SK, Kim MS, Cho EY, Lee JH, Lee KU, et al. Fetal and early postnatal protein malnutrition cause long-term changes in rat liver and muscle mitochondria. J Nutr 2003;133:3085–90.

[10] Reeves PG, Nielsen FH, Fahey GC Jr. AIN-93 purified diets for laboratory rodents: final report of the American Institute of Nutrition ad hoc writing committee on the reformulation of the AIN-76 A rodent diet. J Nutr 1993;123:1939–51.

[11] Borelli P, Blatt S, Pereira J, de Maurino BB, Tsujita M, de Souza AC, et al. Reduction of erythroid progenitors in protein-energy malnutrition. Br J Nutr 2007;97:307–14.

[12] Kratzsch J, Bier H, Klemm R, Pingel H. Radioimmunoassay for the determination of serum cortiscoterone in ducks (Anas platyrhynchos). Arch Exp Veterinārmed 1986;40:531–40.

[13] Seidel B, Bigl M, Franke H, Kittner H, Kiess W, Illes P, et al. Expression of purinergic receptors in the hypothalamus of the rat is modified by reduced food availability. Brain Res 2006;1089:143–52.

[14] Baddeley AJ, Gundersen HJG, Cruz-Orive LM. Estimation of surface area from vertical sections. J Microsc 1986;142:259–76.

[15] Kissmeyer-Nielsen P, Christensen H, Laurberg S. Diverting colostomy induces mucosal and muscular atrophy in rat distal colon. Gut 1994;35:1275–81.

[16] Gundersen HJ, Bagger P, Bendtsen T, Evans SM, Korbo L, Marcussen N, et al. The new stereological tools: disector, fractionator, nucleator and point sampled intercepts and their use in pathological research and diagnosis. APMIS 1988;96:858–81.

[17] Scherle W. A simple method for volumetry of organs in quantitative stereology. Mikroskopie 1970;26:57–60.

[18] Gundersen HJ. The smooth fractionator. J Microsc 2002;207:191–210.

[19] Gundersen HJG. Notes of the estimation of the numerical density of arbitrary profiles: the edge effect. J Microsc 1977;111:219–23.

[20] Vedel-Jensen EB, Gundersen HJG. The rotator. J Microsc 1993;170:35–44.

[21] Gundersen HJG, Jensen EBV, Kieu K, Nielsen J. The efficiency of systematic sampling in stereology – reconsidered. J Microsc 1999;193:199–211.

[22] Giannini EG, Testa R, Savarino V. Liver enzyme alteration: a guide for clinicians. Can Med Assoc J 2005;172:367–79.

[23] Scheig R. Evaluation of tests used to screen patients with liver disorders. Prim Care 1996;23:551–60.

[24] Koyama A, Hashimoto M, Tanaka H, Fujise N, Matsushita M, Miyagawa Y, et al. Malnutrition in Alzheimer's disease, dementia with Lewy Bodies, and frontotemporal lobar degeneration: comparison using serum albumin, total protein, and hemoglobin level. PLoS One 2016;11:E0157053.

[25] Neloska L, Damevska K, Nikolchev A, Pavleska L, Petreska-Zovic B, Kostov M. The association between malnutrition and pressure ulcers in elderly in long-term care facility. Open Access Maced J Med Sci 2016;4:423–7.

[26] Schlaeger R, Haux D, Kattermann R. Studies on the mechanism of the increase in serum alkaline phosphatase activity in cholestasis: significance of the hepatic bile acid concentration for the leakage of alkaline phosphatase from rat liver. Enzyme 1982;28:3–13.

[27] Youssef WI, Tavill AS. Connective tissue diseases and the liver. J Clin Gastroenterol 2002;35:345–9.

[28] Karbalay-Doust S, Noorafshan A. Stereological study of the effects of nandrolone decanoate on the mouse liver. Micron 2009;40:471–5.

[29] Neves RH, Alencar AC, Aguila MB, Mandarim-de-Lacerda CA, Machado-Silva JR, Gomes DC. Hepatic stereology of Schistosomiasis mansoni infected-mice fed a high-fat diet. Mem Inst Oswaldo Cruz 2006;101:253–60.

[30] Altunkaynak BC, Ozbek E. Overweight and structural alterations of the liver in female rats fed a high-fat diet: a stereological and histological study. Turk J Gastroenterol 2009;20:93–103.

[31] Marcos R, Monteiro RAF, Rocha E. Design-based stereological estimation of hepatocyte number, by combining the smooth optical fractionator and immunocytochemistry with anti-carcinoembryonic antigen polyclonal antibodies. Liver Int 2006;26:116–24.

[32] Fasano M, Theise ND, Nalesnik M, Goswami S, Garcia de Davila MT, Finegold MJ, et al. Immunohistochemical evaluation of hepatoblastomas with use of the hepatocyte-specific marker, hepatocyte paraffin 1, and the polyclonal anti-carcinoembryonic antigen. Mod Pathol 1998;11:934–8.

[33] Luna LG. Manual of histologic staining methods of the Armed Forces Institute of Pathology. 3rd ed. New York: McGraw Hill Publishers; 1968.
[34] Carthew P, Edwards RE, Nolan BM. New approaches to the quantitation of hypertrophy and hyperplasia in hepatomegaly. Toxicol Lett 1998;102–103:411–5.
[35] Trotta MR, Cajaiba DM, Parra OM, Dagli ML, Hernandez-Blazquez FJ. Parenteral solution of nutritional hepatotrophic factors improves regeneration in thioacetamide-induced cirrhotic livers after partial hepatectomy. Toxicol Pathol 2014;42:414–21.
[36] Gandillet A, Alexandre E, Holl V, Royer C, Bischoff P, Cinqualbre J, et al. Hepatocyte ploidy in the normal rat. Comp Biochem Physiol A 2003;134:665–73.
[37] Styles JA. Studies on the hyperplastic responsiveness of binucleated hepatocytes. Carcinogenesis 1990;11:1149–52.
[38] Styles JA, Kelly M, Elcombe CR. A cytological comparison between regeneration, hyperplasia and early neoplasia in the rat liver. Carcinogenesis 1987;8:391–9.
[39] Jack EM, Bentley P, Bieri F, Muakkassah-Kelly SF, Stäubli W, Suter J, et al. Increase in hepatocyte and nuclear volume and decrease in the population of binucleated cells in preneoplastic foci of rat liver: a stereolocal study using the nucleator method. Hepatology 1990;11:286–97.
[40] Hsu S, Delgado ER, Otero PA, Teng KY, Kutay H, Meehan KM, et al. MicroRNA-122 regulates polyploidization in the murine liver. Hepatology 2016;64:599–615.
[41] Parra OM, Hernandez-Blazquez FH, De Sousa e Silva RAP, Cunha da Silva JRM, Peduto L, Soares MM, et al. Reduction of liver mass due to malnutrition in rats. Correlation with emaciation of animals and size of organs not inserted in the portal system. Sao Paulo Med J 1995;113:903–9.
[42] Starzl TE, Porter KA, Putnam CW. Intraportal insulin protects from the liver injury of portacaval shunt in dogs. Lancet 1975;2:1241–2.